This article has been accepted for publication in IEEE Control Systems Letters. This is the author's version which has not been fully edited and content may change prior to final publication. Citation information: DOI 10.1109/LCSYS.2022.3204627

Interacting with COVID-19: How population behavior, feedback and memory shaped recurrent waves of the epidemic

Francesco Montefusco[1], Anna Procopio[2], Iulia M. Bulai[3], Francesco Amato[4], Morten G. Pedersen[*,5] and Carlo Cosentino[*,2]

***Abstract*—Until the approval of vaccines at the end of 2020, societies relied on non-pharmaceutical interventions (NPIs) in order to control the COVID-19 pandemic. Spontaneous changes in individual behavior might have contributed to or counteracted epidemic control due to NPIs. For example, the population compliance to NPIs may have varied over time as people developed "epidemic fatigue" or altered their perception of the risk and severity of COVID-19. Whereas official measures are well documented, the behavioral response of the citizens is harder to capture. We propose a mathematical model of the societal response, taking into account three main effects: the citizen response dynamics, the authorities' NPIs, and the occurrence of unpreventable events that significantly alter the virus transmission rate. A key assumption is that a society has a waning memory of the epidemic effects, which reflects on both the severity of the authorities' NPIs and on the citizens' compliance to the prescribed rules. This, in turn, feeds back onto the transmission rate of the disease, such that a higher number of hospitalizations decreases the probability of transmission. We show that the model is able to reproduce the COVID-19 dynamics in terms of hospital admissions for several European countries during 2020 over surprisingly long time scales. Also, it is capable of capturing the effects of disturbances (for example the emergence of new virus variants) and can be exploited for implementing control actions to limit such effects. A possible application, illustrated in the paper, consists of exploiting the estimations based on the data of one country, to predict and control the evolution in another country, where the virus spreading is still in an earlier phase.**

***Index Terms*—Nonlinear model, optimal control, COVID-19.**

I. INTRODUCTION

For most of the first year of the COVID-19 pandemic non-pharmaceutical interventions (NPIs) were the only means to tame the spread of the disease. Societies imposed various control measures ranging from soft recommendations regarding hygiene and face mask use to curfews and hard lockdowns. In the mean time researchers and the pharmaceutical industry worked with incredible efficiency to develop vaccines that became available in late 2020.

NPIs are introduced to change the behavior of the population of a society with the aim to change the course of the epidemic. On the other hand, the dynamics of the epidemic is what motivates institutions to change their response and to decide to impose restrictions. Further, the degree of compliance in the population may change over time as the number of infected cases varies, which could influence the perceived risk of getting infected or modify the perceived severity of the epidemic. Reduced compliance may also be because people begin to show 'pandemic fatigue' for example for economic or psychological reasons [1]. It is thus clear that the dynamics of the epidemic and the behavioral response, both at institutional and personal levels, are intertwined in a feedback loop, which itself may change over time.

Mathematical modeling of COVID-19 has had a tremendous impact on public health measures [2], [3]. For example, to help decision makers the impact of imposing NPIs has been predicted from mathematical modeling [4], [5]. Retrospectively, the effect that NPIs had on disease dynamics has also been studied with the help from models [6]– [9]. However, the structure of these models is typically one-directional: the NPIs are imposed by changing parameters in the models, but, from the best of our knowledge, the feedback from disease dynamics onto the decision process is lacking. In addition, spontaneous behavioral changes in the population are typically not considered, although it is well established that to understand how individuals interact with epidemic diseases mathematical modeling is of great help [10], [11]. Modeling studies that include feedback from the COVID-19 epidemic dynamics onto the transmission rate, in this way modeling behavioral changes, typically consider the feedback to be instantaneous [12], [13]. Another common approach is to model changes in behavioral response by introducing 'switches', where people change their behavior discontinuously between two levels as e.g. the number of infected individuals change [14], [15]. Such mathematical models have been proposed with 'memory' where the switch occurs depending on the incidence levels in a certain time window [14], and further extended to have smooth transitions between the two levels [16]. These latter works did

This work was not supported by any organization

[*] MGP and CC contributed equally to this work.

[1] F. Montefusco is with the Department of Engineering, Università degli Studi di Napoli Parthenope, 80143 Naples, Italy; email: francesco.montefusco@uniparthenope.it

[2] A. Procopio, and C. Cosentino are with the School of Computer and Biomedical Engineering, Università degli Studi Magna Græcia di Catanzaro, 88100 Catanzaro, Italy; email:anna.procopio, carlo.cosentino@unicz.it

[3] I. M. Bulai is with the Dipartimento di Scienze Chimiche, Fisiche, Matematiche e Naturali, Università degli Studi di Sassari, 07100 Sassari, Italy; email:imbulai@uniss.it

[4] F. Amato is with the Department of Electrical Engineering and Information Technology, Università degli Studi di Napoli Federico II, 80125 Napoli, Italy; email:francesco.amato@unina.it

[5] M. G. Pedersen is with the Department of Information Engineering and Department of Mathematics "Tullio Levi-Civita", Università degli Studi di Padova, 35131 Padova, Italy; email:pedersen@dei.unipd.it

not compare the model to COVID-19 data.

We argue that societies during 2020 kept a waning 'memory' of the COVID-19 epidemic. For example, institutions calculate incidence rates, basic reproduction number R_0 values and hospital occupancies from historical and time-averaged data, and decide to introduce or ease restrictions based on such information. Indeed, many countries have semi-automatized the link between epidemic indices and the level of containment measures in effect, but with an inherent delay in the system. It seems also reasonable that the population's perception of the severity of the disease changes with some delay as, for example, the media reports on the epidemic situation.

Consequently, we analyze COVID-19 data until early 2021 (to reproduce a scenario without assuming the effects of vaccine) from several of the most populous western European countries using a modified feedback SIR model with waning memory, where the labels S, I and R represent the different compartments assigned to a population (Susceptible, Infectious, or Recovered). The model incorporates feedback from this social memory onto the transmission rate. Other models, different from the one proposed here, although based on similar principles, have appeared in literature; e.g., Buonomo and Della Marca have developed a model based on information-induced behavioural changes [17] and, more recently, have also studied the effects of vaccine-hesitancy [18] and vaccine-induced relaxation of social-distancing [19]. While in the above papers the authors present a thorough mathematical analysis of the proposed models, the present work is more focused on the model-based analysis of the epidemiological dynamics in different countries, over an extended time interval, and on the optimization of the control strategies in the face of unpreventable disturbances, possibly exploiting similar disturbance-induced effects in the various countries.

Indeed, the model allows us to quantify the effects of the spread in UK of B.1.1.7/Alpha variant, that became dominant at the end of 2020. Then, we exploit this information to predict the trend of the hospital admissions due to the proliferation of this variant in the other investigated European countries, where it became dominant at the end of February/early March 2021. Finally, we show how to employ the model in order to implement control actions that reduce these disturbance effects and maintain the peak value of the new epidemic wave due to the emergence of Alpha variant below a desired threshold.

II. Methods

A. A SIHM model

We consider a SIHM model for characterizing COVID-19 dynamics, where S represents the susceptible individuals, I the infectious, H the cumulative hospital admissions and M the time-weighted average number of hospital admissions (i.e. a memory variable), which feeds back onto the transmission rate of the disease, β_f. The model is described by the equations

$$\dot{S} = -\beta_f SI/N, \quad (1)$$

$$\dot{I} = \beta_f SI/N - (\eta+\alpha) I \quad (2)$$

$$\dot{H} = \eta I \quad (3)$$

$$\dot{M} = (\eta I - M)/\tau \quad (4)$$

with

$$\beta_f = u(1+w)(1-\Delta u), \text{with } u = \frac{\beta}{1+\left(\frac{M}{K_p}\right)^{n_h}}. \quad (5)$$

Here, N is the total number (assumed constant) of individuals in the population; the rate α represents recovery or death of COVID patients that were not hospitalized, while η is the rate of hospital admissions. The transmission rate β_f is determined by i) the feedback function u, which includes both the nominal authorities' NPIs and the citizens' compliance to the prescribed rules (depending on the waning memory variable M); ii) the term w modeling the effects of unpreventable exogenous inputs (i.e. environmental effects/disturbances) significantly altering the disease transmission rate (e.g. the spreading of novel virus variants); iii) the factor Δu representing additional control actions that could be implemented in order to further limit the spread of the epidemic in addition to u. Note that β_f is equal to u when w and Δu are zero; in this case (i.e. $\beta_f = u$) the model describes the "nominal" response of a country to COVID-19: the transmission rate is described by the feedback function u, which is a decreasing function of M with maximal transmission rate β, threshold for the feedback K_p (the value of M needed for 50% transmission rate reduction, i.e. $u = \beta/2$) and exponent n_h determining the steepness of u (when $n_h > 1$, u has a sigmoidal shape whose steepness increases with n_h). The feedback function u allows mimicking the society response to the recent COVID-19 spreading in the country: indeed, a high number of hospital admissions over a time window (determined by the time constant τ of the memory system (see (4)) leads to a rise of M, which decreases the probability of transmission.

Through w the model is capable of taking into account, for example, an increase of mobility with reopening of activities and schools after summer 2020, a lower compliance of the population to the suggested behaviors during the Christmas period or the emergence of new virus variants; therefore, we model w as a piece-wise constant signal denoted by $w^{\{k\}}$, which is composed of k constant subintervals; w_i denotes the constant value in the i-th subinterval, for $i = 1,\ldots,k$, with $w_1 = 0$; the step-wise changes from w_i to w_{i+1}, with $i = 1,\ldots,k-1$, occurs at T_{c_i}, denoting the time of the i-th change of $w^{\{k\}}$; for example, $w^{\{2\}}$ is a piece-wise constant signal composed of 2 subintervals with constant values w_1 and w_2, respectively, characterized by 1 time change at T_{c_1} from w_1 to w_2. Finally, by introducing Δu in (5), we can simulate the results of control strategies aimed at mitigating and anticipating the effects of these environmental disturbances; for example, the model allows us to quantify the consequences on the transmission rate of the emergence of B.1.1.7/Alpha variant in UK, which became dominant at the end of 2020 (see Section III-B); notably, we have exploited this information for predicting the Alpha variant effects in other European countries, where the Alpha variant became dominant a few months later, and for implementing an optimal control action that could be employed in order to reduce these effects, e.g. by maintaining the peak value of the new epidemic wave due

to the emergence of Alpha variant below a desired threshold (see Section III-C).

B. Parameter estimation

We assume that α and η have the same values for all countries; in particular we consider an average time of duration from infection to recovery or death of non-hospitalized cases of 10 days [20]– [23], corresponding to a rate of 0.1/day. Then, if δ represents the percentage of infectious individuals needing hospital admission, we obtain $\alpha = (1-\delta)\times 0.1/\text{day}$, and $\eta = \delta \times 0.1/\text{day}$. We estimate δ from Italian data: about 90k individuals needed hospital admission by the end of July 2020, while an estimation of all infectious individual was about 1.5M by that date [24], which yields $\delta \approx 90k/1.5\text{M} = 0.06$, $\alpha = 0.094/\text{day}$ and $\eta = 0.006/\text{day}$. We use global optimization to estimate the free model parameters providing the best fit to the log-transformed hospital admission data (denoted by $\overline{dH}$) from Germany, France, UK and Italy. For France and Germany, we use weekly hospital admissions: for France, data are available from the week ending March 15th, 2020, while for the Germany from the week ending March 8th, 2020. For Italy and UK, we use daily hospital admissions: for Italy, data are available from February 20th, 2020; for UK, the daily hospital admissions are from March 23rd, 2020 (see Section II-C for link to data sources). For the different countries, we consider data (daily or weekly admissions) until early 2021, in order to reproduce a scenario without assuming the effects of vaccines.

By exploiting the data-set and the devised model, we can estimate the initial value of the unknown number of infectious individuals I_0 at time T_0, which represents the day or week before the first sample (at time T_1) is available for each country, by identifying dH_0, thereby $I_0 = \frac{dH_0}{\eta}$, being η constant and identical for all countries as previously explained.

In the fitting procedure, we assume a piece-wise constant disturbance $w^{\{k\}}$, as defined in the previous section. Note that, at this stage, we do not assume any additional control strategy, thus we set $\Delta u = 0$ in (5). First, we fit the model without any disturbance in (5), i.e. $k = 1$ and $w = w^{\{1\}} = 0$; subsequently, larger values of k are tested according to the procedure illustrated below.

Let us denote by Θ_k the set of optimization parameters, whose cardinality depends on k: for instance, $\Theta_1 = \{I_0, \beta, \tau, K_p, n_h\}$ for $w = w^{\{1\}}$(i.e. no disturbance), $\Theta_2 = \{I_0, \beta, \tau, K_p, n_h, T_{c_1}, w_2\}$ for $w = w^{\{2\}}$, and more in general is $\Theta_k = \{I_0, \beta, \tau, K_p, n_h, T_{c_1}, w_2, \ldots, T_{c_{k-1}}, w_k\}$ for $w = w^{\{k\}}$.

The optimization problem is then defined by

$$\min_{\Theta_k} J, \quad J = \frac{1}{N_D}\sum_j \left(\log dH_j - \log \overline{dH}_j\right)^2, \tag{6}$$

where $\log dH_j$ are the log-transformed simulated daily or weekly hospital admissions (obtained by simulating model (1)–(5)) and $\log \overline{dH}_j$ the log-transformed daily or weekly hospital admissions data, at time j (day or week according to available country data), N_D is the time-series length. In order to minimize the problem defined by (6), i.e. the sum of the squared errors between the log-transformed simulated responses produced by the model and the corresponding log-transformed data, we use a hybrid Genetic Algorithm (GA) that combines the GA with a local gradient-based algorithm [25]. We use the function `ga` from MATLAB$^{\text{TM}}$ (Mathworks, Natick, MA, USA) Global Optimization Toolbox and `fmincon` from MATLAB$^{\text{TM}}$ Optimization Toolbox as the local algorithm. For each value of k, we repeat the GA algorithm six times and select the parameter set that gives the best fitting (i.e. the lowest value of J) as initial condition for the local algorithm. To cope with overfitting, we also compute the Akaike information criterion (AIC) [26], Bayesian information criterion (BIC) [27] and Akaike's final prediction-error criterion (FPE) [28]. Indeed, the cost function J does not take into account the number of optimization parameters (which is equal to $5+2(k-1)$). In general BIC tends to penalize complex models more heavily, on the other hand AIC and FPE tend to choose models which are too complex as the number of data goes to infinity. We exploit the following iterative procedure:

P1) First, compute the scores (J, AIC, BIC, FPE) obtained by SIHM with $w = w^{\{1\}} = 0$.

P2) Then, for each value of k, evaluate the scores obtained using $w = w^{\{k\}}$.

P3) Compare the scores of $w = w^{\{k\}}$ with those obtained by $w = w^{\{k-1\}}$:
if there is an improvement (at least 5%) for each score,
then repeat P2)-P3) with $w = w^{\{k+1\}}$,
else return $w = w^{\{k-1\}}$ as the optimal signal for explaining data.
end

TABLE I
Scores obtained by fitting the dataset for SIHM model for different $w = w^{\{k\}}$ with $k = 1,\ldots,4$. The score highlighted in bold with * means $< 5\%$ improvement obtained by $w = w^{\{k\}}$ with respect to $w = w^{\{k-1\}}$.

Country	Case	Scores			
		J by (6)	AIC	BIC	FPE
Germany	$w = w^{\{1\}}$	0.75	-3.5	5.7	0.930
	$w = w^{\{2\}}$	0.22	-56.5	-43.7	0.290
	$w = w^{\{3\}}$	0.05	-120	-104	0.074
	$w = w^{\{4\}}$	0.04	-126	**-106***	0.065
France	$w = w^{\{1\}}$	0.250	-53	-43.9	0.310
	$w = w^{\{2\}}$	0.055	-116	-104	0.076
	$w = w^{\{3\}}$	0.007	-203	-187	0.011
	$w = w^{\{4\}}$	0.006	**-209***	**-189***	0.010
UK	$w = w^{\{1\}}$	0.270	-383	-364	0.280
	$w = w^{\{2\}}$	0.051	-882	-856	0.053
	$w = w^{\{3\}}$	0.023	-1113	-1080	0.025
	$w = w^{\{4\}}$	**0.022***	**-1123***	**-1082***	**0.024***
Italy	$w = w^{\{1\}}$	0.310	-383	-364	0.320
	$w = w^{\{2\}}$	0.110	-727	-700	0.110
	$w = w^{\{3\}}$	0.038	-1074	-1040	0.040
	$w = w^{\{4\}}$	0.035	**-1098***	**-1056***	0.037

Table I reports the scores by varying k. For each country, the case with $w = w^{\{3\}}$ presents the best trade-off between minimization of J and number of optimization variables: indeed, increasing the number of constant subintervals of w, i.e $w = w^{\{4\}}$, implies at least one score that does not improve $> 5\%$. Tables II and III report the optimal model parameters that provide the best fitting to weekly and daily hospital admissions, respectively, for $w = w^{\{3\}}$. Fig. 1 shows the optimal data interpolation for different $w = w^{\{k\}}$ with $k = 1,2,3$.

TABLE II
Model parameters for weekly hospital admissions for Germany and France. For the optimized parameters, SE represents standard error.

Fixed parameters				
Country	N	T_0 [date]	α [week $^{-1}$]	η [week $^{-1}$]
Germany	83 M	Mar 1	0.094×7	0.006×7
France	67.1 M	Mar 8		

Optimized parameters					
Country	dH_0 (SE) [I. week^{-1}]	β (SE) [week^{-1}]	K_p (SE) [I. week^{-1}]	n_h (SE)	τ (SE) [week]
Germany	23.9 (0.63)	2.5 (0.1)	302 (11.9)	0.98 (0.05)	8.8 (0.12)
France	140 (55.9)	2.89 (0.6)	999 (391)	1.13 (0.24)	9.4 (1.5)

Piece-wise constant disturbance $w = w^{\{3\}}$				
Country	w_2 (SE)	T_{c_1} [date] (SE) [week]	w_3 (SE)	T_{c_2} [date] (SE) [week]
Germany	1.28 (0.09)	Oct 14 (1.95)	4.25 (0.32)	Nov 26 (2.3)
France	0.95 (0.09)	Oct 14 (1.57)	2.12 (0.22)	Dec 9 (1.97)

TABLE III
Model parameters for daily hospital admissions for UK and Italy. For the optimized parameters, SE represents standard error.

Fixed parameters				
Country	N	T_0 [date]	α [day^{-1}]	η [day^{-1}]
UK	66.6 M	Mar 22	0.094	0.006
Italy	60 M	Feb 19		

Optimized parameters					
Country	dH_0 (SE) [I. day^{-1}]	β (SE) [day^{-1}]	K_p (SE) [I. day^{-1}]	n_h (SE)	τ (SE) [day]
UK	1540 (342)	0.27 (0.07)	173 (47.6)	0.62 (0.15)	64 (13.9)
Italy	61.6 (24.7)	0.32 (0.09)	160 (63.9)	1.2 (0.35)	79.8 (32.6)

Piece-wise constant disturbance $w = w^{\{3\}}$				
Country	w_2 (SE)	T_{c_1} [date] (SE) [day]	w_3 (SE)	T_{c_2} [date] (SE) [day]
UK	0.43 (0.04)	Sep 5 (16.2)	1.41 (0.08)	Dec 11 (15.8)
Italy	1.05 (0.08)	Oct 14 (5.95)	2.62 (0.21)	Dec 5 (7.25)

C. Code and data availability

The source code (implemented in Matlab) and data are available at https://github.com/BioMecLabUnicz/Interacting-with-COVID-19-matlab-code.

III. Results and Discussion

A. Model fitting to weekly and daily hospital admissions

The number of identified SARS-CoV-2 positive individuals depends strongly on the amount of testing, which in turn has varied significantly during the COVID-19 epidemic and with great inter-country variability. To avoid the dependence on the testing rate, the results are obtained by fitting weekly or daily hospital admission COVID-19 data. Noteworthy, the number of hospitalizations is also the most critical factor to be considered to assess the capability of the public health systems to cope with the pandemic waves. Moreover, the hospital admission rate represents a significant measure of the severity level of disease and is more closely related to the societal memory state M that affects the transmission rate as defined by (5). The analysis is performed for Germany, France, UK and Italy starting from late February/early March 2020 until January 17th, 2021. According to the iterative procedure described in Section II-B, as reported in Table I, $w = w^{\{3\}}$ is the most suitable signal for reproducing the COVID-19 dynamics for each country in terms of hospital admissions during 2020: Fig. 1 shows how the fitting to data improves significantly going from $w = w^{\{1\}} = 0$ (see solid black curves) to $w = w^{\{2\}}$ (see solid-dashed blue curves) and to $w = w^{\{3\}}$ (see solid-dash-dotted red curves). Parameter estimates for $w = w^{\{3\}}$ are given in Tables II-III. Interestingly, the estimated memory time scale τ is similar for all countries and of the order 61-80 days. The mechanism suggested by the model is that the high number of hospitalizations during March-April 2020 led to severe containment measures, such as lockdowns, and high compliance. The memory of these events likely meant that during the Summer 2020 people only slowly became less compliant and governments only gradually lifted containment measures. However, when people eventually believed that the epidemic was largely under control after 2-3 months with relatively low numbers of hospitalizations and new cases, and/or developed pandemic fatigue in combination with the vacation typically occurring in August (as in Italy and France), the number of cases resurged, which is seen in the number of hospital admission a few weeks later. Thus, for the different countries, the dynamics are well reproduced by assuming two time-changes of the piece-wise constant disturbance w (i.e. $w = w^{\{3\}}$): in general, the first change likely reflects the fact that mobility increased with reopening activities and schools after summer; the second one may correspond to a lower compliance of the population to the suggested behaviors, possibly due to the approaching Christmas period. The first time change T_{c_1} of w occurred on 14 October 2020 for Germany, France and Italy, while for UK the change was early, on 5 September 2021 (see red curves changing from solid to dashed lines at T_{c_1} in Fig. 1): this can be explained by the fact that the lockdown restrictions eased further in UK from 14 August 2020, while the level of the disease was slightly higher than the other countries during the summer with daily hospital admissions that did not drop below an average value of 100; also, the epidemic wave for UK went down more slowly, as modeled by the identified n_h parameter, whose value is lower

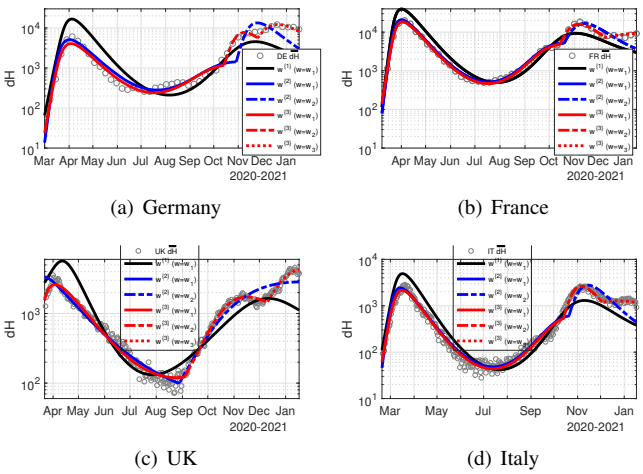

(a) Germany (b) France

(c) UK (d) Italy

Fig. 1. **Best fitting to weekly (Germany and France) and daily (UK and Italy) hospital admissions**. The grey circles represent the data ($\overline{dH}$), the solid black lines the simulated hospital admissions reproduced by the model for $w = w^{\{1\}} = 0$, the solid-dashed blue lines for $w = w^{\{2\}}$ with one step-wise change of w from w_1 (=0) to w_2 at T_{c_1}, the solid-dash-dotted red lines for $w = w^{\{3\}}$ with two step-wise changes of w from w_1 to w_2 at T_{c_1} and from w_2 to w_3 at T_{c_2}; see Table II reporting parameter values for Germany and France and Table III for UK and Italy.

This article has been accepted for publication in IEEE Control Systems Letters. This is the author's version which has not been fully edited and content may change prior to final publication. Citation information: DOI 10.1109/LCSYS.2022.3204627

than the other countries (see Tables II-III). The second time change T_{c_2} of w occurred between the end of November and the beginning of December 2020: in particular on Nov 26 2020 for Germany and on Dec 5 for Italy, on Dec 9 for France, and on Dec 11 for UK (see red curves changing from dashed to dotted lines at T_{c_2} in Fig. 1).

B. Estimation of the piece-wise constant disturbance effects

We exploit the results obtained by the model fitting with $w = w^{\{3\}}$ in order to quantify the effects of the step-wise increases of w on the transmission rate β_f (5). Therefore, we define the factor ρ_i as

$$\rho_i = (1+w_{i+1})/(1+w_i) \tag{7}$$

with $i = 1,2$. Then, ρ_i represents the multiplying factor modifying the transmission rate β_f due to the step-wise change from w_i to w_{i+1}. As previously explained, the step-wise increases w_2 and w_3 reflect an increase of mobility, due to the reopening of the activities after summer 2020 (w_2) and the closeness to Christmas with a lower compliance of the population to the suggested behavior (w_3). For Germany, see Figs. 2(a) and (b), the effects of w_2 and w_3 are similar: both the disturbances determine a rise of β_f by a factor greater than 2 ($\rho_1, \rho_2 > 2$), leading to, respectively, the second peak in Nov 2020 (w_2), and the following one (w_3), after a plateau, in Dec 2020, as shown in Fig. 1(a). For France and Italy, $\rho_2 < \rho_1$: the latter doubles the transmission rate determining the new peak for the second pandemic wave in Nov 2020, while ρ_2 corresponds to a 60-80% increase of β_f, leading to slow down the descending phase of the second wave, as shown in Figs. 1(b) and (d). Note that w_2 exhibits a similar effect on β_f in Germany, France and Italy, resulting in at least doubling the hospitalization rate and a new pandemic wave in autumn 2020. Regarding the third phase (i.e., from the end of Nov 2020), France and Italy exhibit a more limited increase in the transmission rate with respect to Germany, which experienced another hospitalizations peak in Dec 2020: this behavior can be explained by the less stringent lockdown policies actuated in Germany from early Nov 2020 during the second wave, which led to a higher increase of the mobility at the end of Nov 2020 (only from Dec 15, 2020 a hard lockdown was applied in Germany). For UK, we note that the effect of w_2 is lower with respect to the other countries and this can be explained by the fact that mobility was already increased (with rapid easing of lockdown restrictions imposed during the first epidemic wave) resulting in a first wave that went down slowly; consequently, the step-wise increase w_2 identified by the model was lower than in the other countries. Differently from the other countries, for UK $\rho_2 > \rho_1$: the first step-wise increase determines a 40% rise of β_f, leading to the second peak in Nov 2020, whereas w_3 implies a rise of β_f by about 70%, determining the further peak in early 2021, as shown in Fig. 1(c). Taking into account these results, we can assume that the UK transmission rate in the third phase is heavily affected by the emergence of the B.1.1.7/Alpha variant (which became dominant in UK in Dec 2020), determining an additional rise of β_f due to the ratio between ρ_2 and ρ_1, thereby defining $\rho_{Alpha} = \frac{\rho_2}{\rho_1} \approx 1.2$.

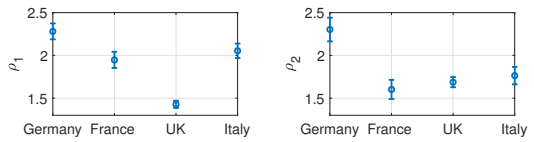

(a) From $w_1 = 0$ to w_2 (b) From w_2 to w_3

Fig. 2. **Effects of the step-wise increases on β_f for the different countries.**

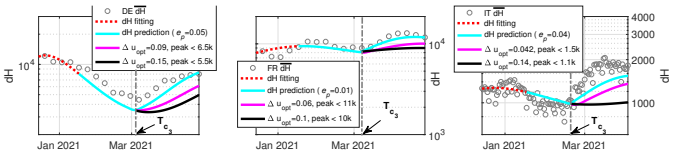

(a) Germany (b) France (c) Italy

Fig. 3. **Model prediction and control action to weekly (Germany and France) and daily (Italy) hospital admissions for containing the effects of Alpha variant**. The grey circles represent the data ($\overline{dH}$), the dotted red curves the fitting results obtained by the devised model with $w = w^{\{3\}}$ as shown in Fig. 1, the cyan curves the prediction of the model with a new step-wise change at T_{c_3} simulating Alpha variant effects (e_p, reported in the legend, represents the prediction error obtained by computing the distance of the simulated curve from data as performed by (6)). The magenta and black curves simulate the implementation of two possible control actions with the aim to maintain the peak of the following wave below a desired value.

C. Prediction of the effects of Alpha variant and relative control action for France, Germany and Italy

We use the model parameters obtained by fitting the data until Jan 17, 2021, and predict the following trend of hospital admissions for France, Germany and Italy with the aim to show how the model is able to reproduce the new epidemic wave due to Alpha variant. In particular, we introduce a new step-wise increase w_4 at time T_{c_3}, where w_4 is computed by exploiting the factor ρ_{Alpha} obtained from UK data ($\rho_{Alpha} = (1+w_4)/(1+w_3)$, i.e. $w_4 = \rho_{Alpha}(1+w_3) - 1$). For each country, T_{c_3} is obtained by looking at the time where Alpha variant became dominant (available at https://www.gisaid.org/hcov19-variants/), in particular at the end of Feb 2021 for Italy, and at the beginning of Mar 2021 for France and Germany. Fig. 3 shows how the model is able to predict well the hospital admissions data from Jan 17, 2021 to the new peak due to emergence of Alpha variant for each country (see cyan curves). Then, we implement a control strategy by minimizing the following cost function with respect to Δu:

$$f = \sum_j k_a (\Delta u)^2 + \frac{k_b}{\left(\min\left(\log dH_j - k_{wd}(p_{max} - 100), 0\right)\right)^2}, \tag{8}$$

where k_a and k_b are weight coefficients, $(p_{max} - 100)$ represents the maximum value of the peak and k_{wd} is a constant equal to 1 for daily data or 7 for weekly data. By solving (8), we achieve the optimal control input Δu, a step-wise signal to be applied at T_{c_3}, that maintains the peak of the new epidemic wave due to Alpha variant below a limit value (i.e. $k_{wd}(p_{max} - 100)$). Fig. 3 shows two possible control actions to be implemented for each country in order to keep the peak

value below the desired threshold (see magenta and black curves).

IV. Conclusions

Our work presents a simple model incorporating feedback and memory into a SI(R) model capable of capturing COVID-19 dynamics during 2020 over surprisingly long time scales. The severity of the epidemic, which feed backs on the transmission rate, is measured by a weighted average of hospital admissions with waning memory. One could use e.g. daily deaths due to COVID-19 or other measures of the state of the epidemic as an alternative variable controlling the memory variable. Our results suggest that the memory time scales of the societies were approximately 60-80 days, i.e., the feedback is mostly influenced by the number of hospitalizations, whether high or low, in the previous $\sim$2 months.

Besides allowing us to quantify the effects of possible disturbances altering the transmission rate as, for example, changes in perceived disease severity or pandemic "fatigue", the model permits quantifying and controlling the emergence of new virus variants. For example, we have shown how the insights provided by the model on the effects of Alpha variant in UK can be exploited by the other European countries through the implementation of control actions able to limit the next wave peak.

Note that the model does not treat regional differences within each country, although such heterogeneity is well known to be relevant. Further studies could apply our approach to regional data, which however suffer from "noise" due to isolated outbreaks. In addition, national health orders and public compliance were often based on the national situation. Thus, a hierarchical model that considers both regional and national COVID-19 dynamics would be needed.

References

[1] S. Reicher and J. Drury, "Pandemic fatigue? how adherence to COVID-19 regulations has been misrepresented and why it matters," *BMJ*, vol. 372, p. n137, Jan 2021.

[2] G. Giordano *et al.*, "Modelling the COVID-19 epidemic and implementation of population-wide interventions in Italy," *Nat Med*, vol. 26, no. 6, pp. 855–860, 06 2020.

[3] E. Brooks-Pollock, L. Danon, T. Jombart, and L. Pellis, "Modelling that shaped the early COVID-19 pandemic response in the UK," *Philos Trans R Soc Lond B Biol Sci*, vol. 376, no. 1829, p. 20210001, 07 2021.

[4] N. Ferguson *et al.*, "Report 9: Impact of non-pharmaceutical interventions (NPIs) to reduce COVID-19 mortality and healthcare demand," Imperial College London, Tech. Rep., 2020.

[5] N. G. Davies *et al.*, "Effects of non-pharmaceutical interventions on COVID-19 cases, deaths, and demand for hospital services in the UK: a modelling study," *Lancet Public Health*, vol. 5, no. 7, pp. e375–e385, 07 2020.

[6] J. Dehning *et al.*, "Inferring change points in the spread of COVID-19 reveals the effectiveness of interventions," *Science*, May 2020.

[7] J. M. Brauner *et al.*, "Inferring the effectiveness of government interventions against COVID-19," *Science*, vol. 371, no. 6531, 02 2021.

[8] T. Mitze, R. Kosfeld, J. Rode, and K. Wälde, "Face masks considerably reduce COVID-19 cases in Germany," *Proc Natl Acad Sci U S A*, vol. 117, no. 51, pp. 32 293–32 301, 12 2020.

[9] M. G. Pedersen and M. Meneghini, "Data-driven estimation of change points reveals correlation between face mask use and accelerated curtailing of the first wave of the COVID-19 epidemic in Italy," *Infect Dis (Lond)*, vol. 53, no. 4, pp. 243–251, 04 2021.

[10] S. Funk, M. Salathé, and V. A. A. Jansen, "Modelling the influence of human behaviour on the spread of infectious diseases: a review," *J R Soc Interface*, vol. 7, no. 50, pp. 1247–56, Sep 2010.

[11] F. Verelst, L. Willem, and P. Beutels, "Behavioural change models for infectious disease transmission: a systematic review (2010-2015)," *J R Soc Interface*, vol. 13, no. 125, 12 2016.

[12] G.-H. Li and Y.-X. Zhang, "Dynamic behaviors of a modified SIR model in epidemic diseases using nonlinear incidence and recovery rates," *PLoS One*, vol. 12, no. 4, p. e0175789, 2017.

[13] E. Franco, "A feedback SIR (fSIR) model highlights advantages and limitations of infection-dependent mitigation strategies," *arXiv*, no. 2004.13216, 2020.

[14] Z. Chladná, J. Kopfová, D. Rachinskii, and S. C. Rouf, "Global dynamics of SIR model with switched transmission rate," *J Math Biol*, vol. 80, no. 4, pp. 1209–1233, 03 2020.

[15] T. Odagaki, "Self-organized wavy infection curve of COVID-19," *Sci Rep*, vol. 11, no. 1, p. 1936, 01 2021.

[16] M. te Vrugt, J. Bickmann, and R. Wittkowski, "Containing a pandemic: nonpharmaceutical interventions and the 'second wave'," *Journal of Physics Communications*, vol. 5, no. 5, p. 055008, 2021.

[17] B. Buonomo and R. Della Marca, "Effects of information-induced behavioural changes during the COVID-19 lockdowns: the case of Italy," *Royal Society Open Science*, vol. 7, no. 10, p. 201635, oct 2020.

[18] B. Buonomo, R. Della Marca, A. d'Onofrio, and M. Groppi, "A behavioural modelling approach to assess the impact of COVID-19 vaccine hesitancy," *Journal of Theoretical Biology*, vol. 534, p. 110973, feb 2022.

[19] B. Buonomo, R. Della Marca, and S. S. Sharbayta, "A behavioral change model to assess vaccination-induced relaxation of social distancing during an epidemic," *Journal of Biological Systems*, vol. 30, no. 01, pp. 1–25, mar 2022.

[20] Q. Li *et al.*, "Early transmission dynamics in Wuhan, China, of novel coronavirus-infected pneumonia," *N Engl J Med*, vol. 382, no. 13, pp. 1199–1207, 03 2020.

[21] S. A. Lauer *et al.*, "The incubation period of coronavirus disease 2019 (COVID-19) from publicly reported confirmed cases: Estimation and application," *Ann Intern Med*, vol. 172, no. 9, pp. 577–582, May 2020.

[22] Y. Bai *et al.*, "Presumed asymptomatic carrier transmission of COVID-19," *JAMA*, vol. 323, pp. 1406–1407, Feb 2020.

[23] A. Sakurai *et al.*, "Natural history of asymptomatic SARS-CoV-2 infection," *N Engl J Med*, vol. 383, no. 9, pp. 885–886, 08 2020.

[24] National Institute of Statistics, Rome, Italy., "Primi risultati dell'indagine di sieroprevalenza sul Sars-CoV-2," National Institute of Statistics, Rome, Italy., Tech. Rep., 2020. [Online]. Available: https://www.istat.it/it/files//2020/08/ReportPrimiRisultatiIndagineSiero.pdf

[25] D. E. Goldberg, *Genetic Algorithms in Search, Optimization and Machine Learning*. Boston: Addison-Wesley, 1989.

[26] H. Akaike, "A new look at the statistical model identification," *IEEE Transactions on Automatic Control*, vol. 19, pp. 716–723, 1974.

[27] G. E. Schwarz, "Estimating the dimension of a model," *Annals of Statistics*, vol. 6, no. 2, pp. 461–464, 1978.

[28] L. Ljung, *System Identification: Theory for the User*. Prentice Hall, 1999.